

Exponential localization of moving-end mirror in an optomechanical system

Kashif Ammar Yasir*,¹ Muhammad Ayub,^{1,2} and Farhan Saif¹

¹*Department of Electronics, Quaid-i-Azam University, 45320, Islamabad, Pakistan.*

²*LINAC Project, PINSTECH, Nilore, 45650, Islamabad, Pakistan.*

We discuss the dynamics of moving end mirror of an optomechanical system that consists of a Fabry-Perot cavity loaded with dilute condensate and driven by a single mode optical field. It is shown that quantum mechanical phenomenon of dynamical localization occurs both in position and momentum space for moving end mirror in the system. The parametric dependencies of dynamical localization are discussed. We also provide a set of parameters which makes this phenomenon experimentally feasible.

Keywords: optomechanics, Bose-Einstein condensate, dynamical localization

I. INTRODUCTION

Cavity-optomechanics deals with the interaction of an optical field in a resonator with confining mirrors [1]. Recent experimental advances make it possible to couple cold atoms and Bose-Einstein condensates (BEC), mechanical membrane and nano-sphere with the optomechanical systems [2]. Hence, these hybrid-opto mechanical systems are playground to study phenomena related to mirror-field interaction, and atom-field interaction which provide founding principles to develop numerous sensors, and devices in quantum metrology [3, 4]. In opto-mechanics the mechanical effects of light lead to cooling the motion of a movable mirror to its quantum mechanical ground state [5–7], and to observe strong coupling effects [8–10]. In earlier work optomechanical systems were proposed precision measurement in gravitational wave detectors [11] and to measure displacement with large accuracy [12], and recently the development of optomechanical crystals [13]. Recent theoretical discussions and simulations on bistable behavior of BEC-optomechanical system [14], high fidelity state transfer [15, 16], steady-state entanglement of BEC and moving end mirror [17, 18], macroscopic tunneling of an optomechanical membrane [19] and role reversal between matter-wave and quantized light field are guiding towards new avenues in cavity optomechanics. In this submission we report the classical and quantum dynamics in position and momentum space and show that dispersion is suppressed in quantum domain while classical [20, 21] counterpart increases with time following a power-law. This contrasting behavior is an analog of Anderson localization and termed as dynamical localization or exponential localization [22]. Dynamical localization is studied in periodically driven nonlinear systems [23–28] and provides quantum mechanical limits on classical diffusion of wave packet. The phenomenon of dynamical localization emerges in the explicitly time dependent system. The single mode laser field excite condensate atoms to momentum side modes which behave formally like a moving

mirror driven by the radiation force of intra-cavity field. The side modes induce phase modulation to the field [29], which provide modulation to the radiation pressure exerted on mirror [30]. In this paper, the model of the system is presented in section II. In section III, we derive the Langevin equation and in section IV, we explain dynamical localization of the condensates in the system. In section V, we explain dynamical localization as a function of modulation amplitudes.

II. THE MODEL

We consider a Fabry-Pérot cavity of length L with a moving end mirror driven by a single mode optical field of frequency ω_p and BEC with N-two level atoms trapped in an optical lattice potential [31, 32]. Moving end mirror has harmonic oscillations with frequency ω_m and exhibits Brownian motion in the absence of coupling with radiation pressure.

The Hamiltonian of BEC-optomechanical system is,

$$\hat{H} = \hat{H}_m + \hat{H}_a + \hat{H}_T, \quad (1)$$

where, \hat{H}_m describes the intra-cavity field and its coupling to the moving end mirror, \hat{H}_a accounts for the BEC and its coupling with intra-cavity field while, \hat{H}_T accounts for noises and damping associated with the system. The Hamiltonian \hat{H}_m is given as [33],

$$\hat{H}_m = \hbar\Delta_c\hat{c}^\dagger\hat{c} + \frac{\hbar\omega_m}{2}(\hat{p}^2 + \hat{q}^2) - \xi\hbar\hat{c}^\dagger\hat{c}\hat{q} - i\hbar\eta(\hat{c} - \hat{c}^\dagger), \quad (2)$$

where, first term is free energy of the field, $\Delta_c = \omega_c - \omega_p$ is detuning, here, ω_c is cavity frequency and \hat{c}^\dagger (\hat{c}) are creation (annihilation) operators for intra-cavity field interacting with mirror and condensates and their commutation relation is $[\hat{c}, \hat{c}^\dagger] = 1$. Second term represents energy of moving end mirror. Here \hat{q} and \hat{p} are dimensionless position and momentum operators for moving end mirror, such that, $[\hat{q}, \hat{p}] = i$. Intra-cavity field couples BEC and moving end mirror through radiation pressure. When n photons interacts with the surface of mirror in cavity round trip time $t = 2L/c$, c represents speed of

*kashif.ammar@yahoo.com

light and L is cavity length, and transfer $2\hbar k$ momentum to moving end mirror, here $k = \omega_c/c$. Therefore, the radiation pressure force $\hat{c}^\dagger \hat{c} \hbar \omega_c / L$ will change the position \hat{q} of moving end mirror and couples moving end mirror with intra-cavity field. Third term represents this coupling and $\xi = \sqrt{2}(\omega_c/L)x_0$ is the coupling strength where, $x_0 = \sqrt{\hbar/2m\omega_m}$, is zero point motion of mechanical mirror of mass m . Last term gives relation of intra-cavity field and output power $|\eta| = \sqrt{P\kappa/\hbar\omega_p}$, where, P is the input laser power and κ is cavity decay rate associated with outgoing modes.

Now the Hamiltonian for BEC and intra-cavity field and their coupling is derived by considering quantized motion of atoms along the cavity axis in one dimensional model. We assume that BEC is dilute enough and many body interaction effects are ignored [14]. We have

$$\hat{H}_a = \frac{\hbar U_0 N}{2} \hat{c}^\dagger \hat{c} + \frac{\hbar \Omega}{2} (\hat{P}^2 + \hat{Q}^2) + \xi_{sm} \hbar \hat{c}^\dagger \hat{c} \hat{Q} \quad (3)$$

here, first term describes energy of field due to the condensate. Second term expresses the energy of the condensate in the cavity following harmonic motion. Here, $\hat{P} = \frac{i}{\sqrt{2}}(\hat{b} - \hat{b}^\dagger)$ and $\hat{Q} = \frac{1}{\sqrt{2}}(\hat{b} + \hat{b}^\dagger)$ are dimensionless momentum and position operators for condensate which are related as $[\hat{Q}, \hat{P}] = i$ and $\Omega = 4\omega_r$ where, $\omega_r = \hbar k^2 / 2m_a$ is recoil frequency of an atom associated with the change in energy due to absorption or emission of a single photon. Last term in equation (3) describes coupling energy of field and condensate with coupling strength $\xi_{sm} = \frac{\omega_c}{L} \sqrt{\hbar/m_{sm}4\omega_r}$, where, $m_{sm} = \hbar\omega_c^2 / (L^2 N U_0^2 \omega_r)$ is the effective mass of side mode which shows that side mode formally behave like a mirror whose motion is driven by interacting radiation pressure.

III. LANGEVIN EQUATIONS

The Hamiltonian \hat{H}_T accounts for the effects of dissipation in the intra-cavity field, damping of moving end mirror and depletion of BEC in the system via standard quantum noise operators [34]. The total Hamiltonian H leads to coupled quantum Langevin equations for position and momentum of moving end mirror and BEC, viz.,

$$\frac{d\hat{c}}{dt} = \dot{\hat{c}} = (i\tilde{\Delta} + i\xi\hat{q} - i\xi_{sm}\hat{Q} - \kappa)\hat{c} + \eta + \sqrt{2\kappa a_{in}} \quad (4)$$

$$\frac{d\hat{p}}{dt} = \dot{\hat{p}} = -\omega_m \hat{q} + \xi \hat{c}^\dagger \hat{c} - \gamma'_m \hat{p} + \hat{f}_B, \quad (5)$$

$$\frac{d\hat{q}}{dt} = \dot{\hat{q}} = \omega_m \hat{p}, \quad (6)$$

$$\frac{d\hat{P}}{dt} = \dot{\hat{P}} = -4\omega_r \hat{Q} - \xi_{sm} \hat{c}^\dagger \hat{c} - \gamma_{sm} \hat{P} + \hat{f}_{1m}, \quad (7)$$

$$\frac{d\hat{Q}}{dt} = \dot{\hat{Q}} = 4\omega_r \hat{P} - \gamma_{sm} \hat{Q} + \hat{f}_{2m}. \quad (8)$$

In above equations $\tilde{\Delta} = \Delta_c - NU_0/2$, whereas \hat{a}_{in} is Markovian input noise of the cavity field. The term γ'_m gives mechanical energy decay rate of the moving end mirror and \hat{f}_B is Brownian noise operator [35, 36]. The term γ_{sm} represents damping of BEC due to harmonic trapping potential which effects momentum side modes while, \hat{f}_{1m} and \hat{f}_{2m} are the associated noise operators assumed to be Markovian.

To consider the classical dynamics, we consider positions and momenta as classical variables. In the steady state, we use adiabatic approximation in which we set time derivative of the field as zero in equation(4). The steady state field defined as

$$\alpha = \frac{\eta}{\kappa + i(\Delta_a - \xi q + \xi_{sm} Q)}. \quad (9)$$

Here, $\hat{c} \rightarrow \alpha$ is the classical limit. We use this relation in equations (5,7) and put these equations in the second derivative of equations (6,8). As a result the coupled equations of motion for the moving end-mirror and BEC reveal their coupled nonlinear dynamics, that is,

$$\frac{d^2 q}{dt^2} = -\omega_m^2 q + \frac{\omega_m \xi \eta^2}{\kappa^2 + (\tilde{\Delta} + \xi q - \xi_{sm} Q)^2}, \quad (10)$$

$$\frac{d^2 Q}{dt^2} = -4\omega_r^2 Q - \frac{4\omega_r \xi_{sm} \eta^2}{\kappa^2 + (\tilde{\Delta} + \xi q - \xi_{sm} Q)^2}. \quad (11)$$

Now we describe Hamiltonian as $H = K + V$ where, K is kinetic energy of the system and the potential energy V is obtained from equation (10). We further assume that $\xi_{sm} \ll \xi$ which provides the BEC evolution as harmonic oscillator with frequency $4\omega_r$, such that, $Q = Q_0 \cos(4\omega_r t)$, where, Q_0 is the maximum displacement of BEC from mean position. We introduce some dimensionless parameters defined as, $\gamma = \omega_m/\omega_r$, $\beta = \eta^2/\kappa^2$, $\mu = \Delta/\kappa$, $\mu_1 = \xi/\kappa$, $\lambda = \frac{\xi_{sm}}{\xi} Q_0$ where, $Q_0 = Q_1/\lambda_p$ and using dimensionless time, $\tau = \omega_r t$. By using above parameters and integrating equation (10) we get,

$$V = \frac{dq}{d\tau} = \frac{1}{2} \gamma^2 q^2 - \int \frac{\gamma \xi \beta / \omega_r}{1 + [\mu + \mu_1 \{q - \lambda \cos(4\tau)\}]^2} dq \quad (12)$$

Now, we can write Hamiltonian H ,

$$H = -\frac{\partial^2}{2\partial q^2} + \frac{1}{2} \gamma^2 q^2 - \int \frac{\gamma \xi \beta / \omega_r}{1 + [\mu + \mu_1 \{q - \lambda \cos(4\tau)\}]^2} dq \quad (13)$$

By using transformation $x = Q - \lambda \cos(4\tau)$, we find an effective Hamiltonian for the mirror, that is,

$$H_{eff} = \frac{1}{2} \tilde{p}^2 + \frac{1}{2} x^2 + x \lambda_{eff} \cos(4\tau) - \gamma_m \beta \arctan(\mu - \mu_1 x), \quad (14)$$

where, $\gamma_m = \frac{4\xi}{\gamma\omega_m}$ and $\lambda_{eff} = (1 + \frac{32}{\gamma^2})\lambda$ is the effective modulation.

In our later work we consider the power of external field $P = 0.0164$ mW with frequency $\omega_p = 3.8 \times 2\pi \times 10^{14}$ Hz

and wave length $\lambda_p = 780$ nm. Coupling of external field and intra-cavity field is $\eta = 18.4 \times 2\pi$ MHz and frequency of intra-cavity field is considered $\omega_c = 15.3 \times 2\pi \times 10^{14}$ Hz which produces recoil of $\omega_r = 3.8 \times 2\pi$ kHz in atoms placed in cavity of length $l = 1.25 \times 10^{-4}$ m and having decay rate $\kappa = 1.3 \times 2\pi$ MHz. Moving end mirror of cavity should be perfect reflector that oscillates with a frequency $\omega_m = \omega_r/\hbar = 15.2 \times 2\pi$ kHz. The mirror-field and condensate-field coupling strengths are, respectively, $\xi = 15.07$ MHz and $\xi_{sm} = 14.39$ kHz. Detuning of the system is taken as $\Delta = \Delta_c + \frac{U_0 N}{2} = 0.52 \times 2\pi$ MHz, where vacuum Rabi frequency of the system is $U_0 = 3.1 \times 2\pi$ MHz and number of ultra cold atoms placed in the BEC-optomechanical system are $N = 2.8 \times 10^4$ [2, 38–41]. These experimental parameters are used to obtain numerical results presented in all the figures.

IV. DYNAMICAL LOCALIZATION OF MIRROR

In order to discuss classical dynamics, we solve Hamilton's equations and in quantum domain, we solve time dependent Schrödinger equation. The classical dynamics of mirror is studied by Poincaré surfaces of section for different modulation amplitudes. Fig-1 shows Poincaré sur-

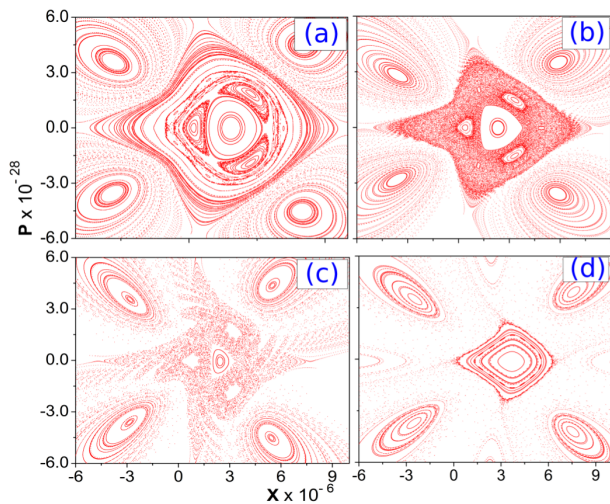


FIG. 1: Phase Space (Poincaré surface of section) plots of moving end mirror for different effective modulation amplitudes $\lambda_{eff} = 2.6 \times 10^{-6}m, 5.2 \times 10^{-6}m, 1.05 \times 10^{-5}m, 3.15 \times 10^{-5}m$ in figure (a), (b), (c) and (d), respectively. Where, $\mu = -0.4, \mu_1 = 2, \beta = 1.8$ and $\gamma_m = 0.6034$.

faces of section for 500 initial position of the mirror. For sufficiently large modulation classical phase space shows mixed behavior i.e. stable islands are emerged in chaotic regions. We note that chaotic regions increase with the modulation amplitude while resonant regions shrink. As dynamical localization emerges from quantum evolution of wave packet in classically chaotic regime, we study the behavior of momentum and position dispersion of movable mirror for modulation amplitude showing mixed

phase space behavior. The quantum dynamics of the mirror is explored by evolving a Gaussian wave packet, $\Psi(x)$, defined at $\tau = 0$,

$$\Psi(x) = \frac{1}{\sqrt{\sqrt{2\pi}\Delta x}} \exp\left(-\frac{(x-x_0)^2}{2\Delta x^2}\right) \times \exp\left(-i\frac{p_0 x}{\hbar}\right), \quad (15)$$

where, initial dispersion in position and momentum is defined in such a way that it satisfy the minimum uncertainty condition. For all numerical calculations, we use $\Delta x = 1, \Delta p = 0.5$ and scaled Planck's constant is $\hbar = 1$. Whenever classical parameters are evaluated for comparison, we use a Gaussian ensemble with the same initial dispersion in position and momentum and initially placed with same mean position and momentum as in the case of quantum wave packet. Fig 2 shows classical and quantum

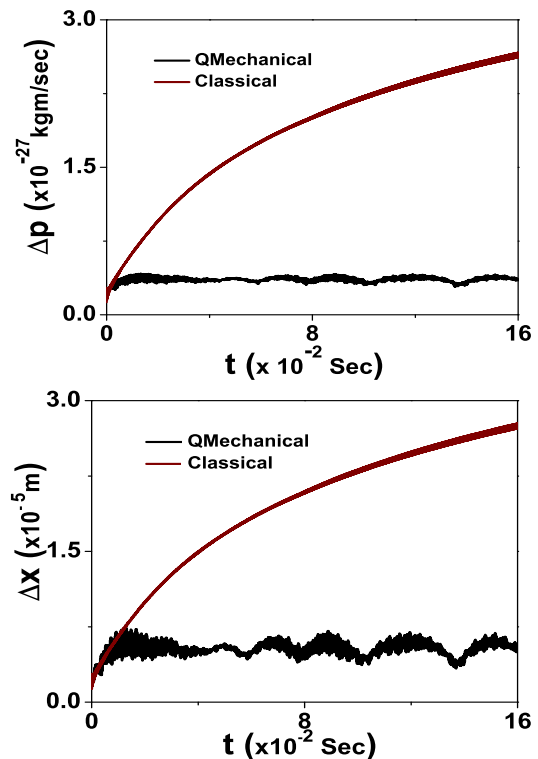


FIG. 2: Classical and quantum dispersion in position, Δx (upper figure) and momentum Δp , (lower figure) of movable vs time at $\lambda_{eff} = 1.05 \times 10^{-5}m$. The remaining parameters are the same as in Fig-1.

dispersion in position and momentum space as a function of time. The dispersion in momentum space follow classical diffusion for quantum break time $t \sim 12.7$ msec and after this time $t > 12.7$ msec, the quantum mechanical dispersion of mirror in momentum space becomes saturated and oscillate around a mean value. While classical dispersion increases continuously with time, following t^α law, where $\alpha = 0.6$ showing anomalous diffusion in classical domain. Similarly, quantum dispersion in position space initially diffuses for quantum break time $t \sim 23.7$ msec and later saturates and show small oscillations around mean value whereas, classical dispersion

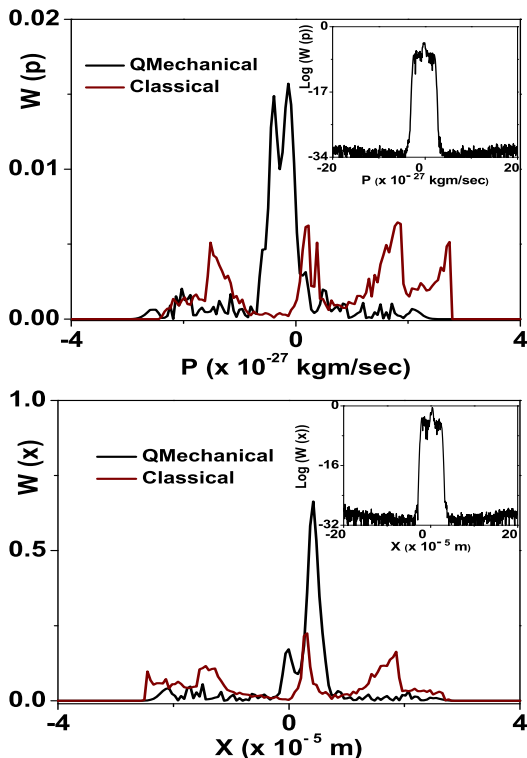


FIG. 3: Classical and quantum mechanical momentum distribution at time $t = 131.5 \text{ msec}$ in momentum space $W(p)$ (upper figure) and position space $W(x)$ (lower figure). The insets show exponential localization behaviour in distribution on logarithm scale. The remaining parameters are the same as in Fig-1.

in position space follows a continues diffusion even after the quantum break time. The suppression in quantum dispersion in position and momentum space is a signature of dynamical localization of mirror in position and momentum space [42]. We study position and momentum distribution of the wave packet for $t = 131.5 \text{ msec}$ which is a time at which dispersion in position and momentum is dynamically localized. Fig-3 shows classical and quantum mechanical time averaged probability distribution of mirror both in position, $W(x) = |\Psi(x)|^2$ and momentum space $W(p) = |\Psi(p)|^2$. The inset show the quantum results in log scale. These results show that classical probability distribution in position and momentum space is broader than the quantum mechanical distribution. Classical probability distribution in position and momentum space is almost equally distributed over the entire space. While, quantum mechanical probability distribution both in position and momentum space is maximum near $x = 1$. The peaks appearing in quantum mechanically position and momentum distribution are due to stable islands in the chaotic sea as shown in Fig-1. The quantum mechanical distribution of wave packet in position and momentum space at large time $t = 131.5 \text{ msec}$ is confirmation of dynamical localization of the mirror. The spatiotemporal behavior of mirror

for $\lambda_{eff} = 4$ is shown in Fig-4 for the same parameters as in Fig-2. The time evolution of probability distribution of quantum wave packet shows localization effects both in position and momentum beyond quantum break time. The quantum probability distribution in position and momentum space remains localized with small fluctuations in position and momentum space while, in classical domain distributions show ever spreading behavior in position and momentum space.

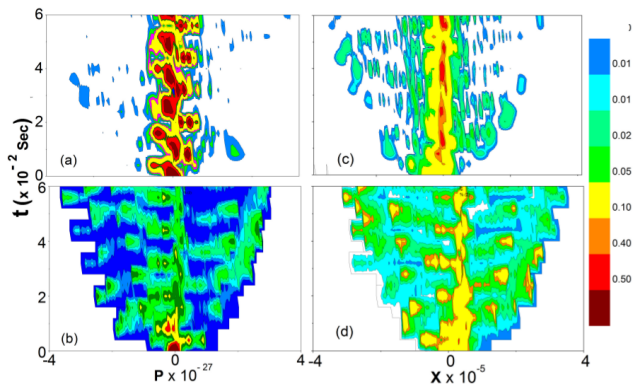


FIG. 4: Spatio-temporal dynamics of mirror in momentum and position space vs time shows: (a) quantum mechanical probability distribution in momentum space, (b) classical distribution in momentum space, (c) quantum mechanical probability distribution in position space, and (d) classical distribution in position space. The remaining parameters are the same as in Fig-1.

V. EFFECTS OF MODULATION

In this section, we study the effects of modulation on the position and momentum dispersion of movable mirror. Fig-5 shows effects of modulation on classical and quantum dispersion of the mirror in position and momentum space. The classical ensemble or quantum wave packet is evolved for $t = 131.5 \text{ msec}$ for fixed rescaled Planck's constant $\hbar = 0.1, 1$ and dispersion at $t = 131.5 \text{ msec}$ is plotted versus fixed effective modulation. We observe that when there is no modulation, classical and momentum dispersions show not a significant difference both in position and momentum space. But as effective modulation increases, the quantum dispersion shows dynamical localization effects while classical dispersion in position and momentum shows diffusion. The localization effects appear for the effective modulation where corresponding classical phase space is mixed. For small effective modulation, corresponding phase space is near integrable and no dynamical localization effects appear while for large λ_{eff} , localization effects are seen. We get strong dynamical localization at that particular effective modulations where the difference between classical dispersion and quantum mechanical dispersion is

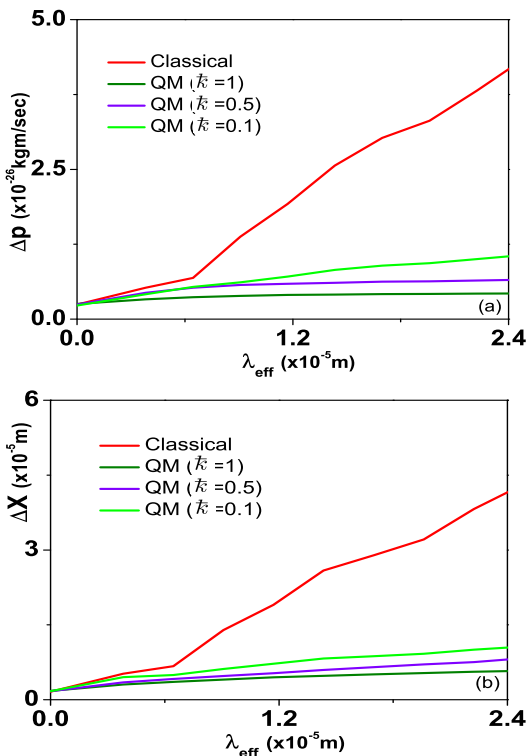


FIG. 5: Dispersion in momentum and position space vs modulation at $t = 131.5 msec$. Upper figure shows the behavior of momentum dispersion vs effective modulation amplitude λ_{eff} while lower figure shows the behavior of position dispersion vs λ_{eff} . Quantum dispersion behavior is plotted for rescaled Planck's constant $\hbar = 0.1, 0.5, 1$. The remaining parameters are the same as in Fig. 1

maximum and vice versa is also true.

The Fig-5 also shows behavior of quantum dispersion in position and momentum space for different values of effective Planck's constant, \hbar . As \hbar is decreased curve representing quantum dispersion approaches to the curve showing classical dispersion which is a manifestation of correspondence principle.

VI. CONCLUSION

We conclude that the motion of moving end mirror weakly coupled with Bose-Einstein condensate in the optomechanical cavity (Fabry-Perot Cavity) shows dynamical localization in position and momentum space. Moreover, for increasing modulation dynamical localization in momentum space doesn't disappear as in the case of driven optical lattice [26] where this localization effect is governed by Bessel function with modulation strength as argument of Bessel function and dynamical localization revives for the value of arguments where Bessel function is zero. In position space, localization length slowly increases with modulation as shown in the Fig-5. The set of parameters used here makes this phenomenon experimentally feasible.

-
- [1] T. J. Kippenberg and K. J. Vahala, *Science* **321**, 1172 (2008).
- [2] F. Brennecke, S. Ritter, T. Donner, and T. Esslinger, *Science* **322**, 235 (2008).
- [3] F. Saif: Recurrence Tracking Microscope. *Phys. Rev. A* **73**, 033618 (2006).
- [4] F. Saif: Optimal Quantum Clocks based on Wave Packet Recurrences. *J. of Russ. Laser Res.* **30**, 242-246 (2009).
- [5] A. D. O'Connell et. al, *Nature* 464, 697 (2010).
- [6] J. D. Teufel et. al, *Nature* 475, 359 (2011).
- [7] J. Chan et. al, *Nature* 478, 89 (2011).
- [8] S. Groblacher, K. Hammerer, M.R. Vanner, and M. Aspelmeyer, *Nature (London)* 460, 724 (2009).
- [9] J. D. Teufel, D. Li, M. S. Allman, K. Cicak, A. J. Sirois, J. D. Whittaker, and R. W. Simmonds, *Nature (London)* 471, 204 (2011).
- [10] E. Verhagen, S. Deleglise, S. Weis, A. Schliesser, and T. J. Kippenberg, *Nature (London)* 482, 63 (2012).
- [11] V. Braginsky and S. P. Vyatchanin, *Phys. Lett. A* **293**,329 (2002).
- [12] D. Rugar et al., *Nature (London)*, **430**, 329 (2004).
- [13] M. Echenfield et al., *Nature* 462, 78, (2012).
- [14] K. Zhang, W. Chen, M. Bhattacharya, and P. Meystre, *Phys. Rev. A* **81**, 013802 (2010).
- [15] Ying-Dan Wang and A. A. Clerk, *Phys. Rev. Lett.* 108, 153603, (2012).
- [16] S. Singh et al., *Phys. Rev. A* **86**, 021801, (2012).
- [17] M. Asjad, and F. Saif, *Phys. Rev. A* **84**, 033606 (2011).
- [18] M. Asjad, and F. Saif: Engineering Entanglement mechanically. *Phys. Lett. A* **376**, 2608-2612 (2012).
- [19] L. F. Buchmann et al., *Phys. Rev. Lett.* 108, 210403 (2012).
- [20] Yang, C., Wu, Q.: On stability analysis via Lyapunov exponents calculated from a time series using nonlinear mapping—a case study. *Nonlinear Dyn.* **59**, 239257 (2010).
- [21] Zhang, X., Zhu, H., Yao, H.: Analysis of a new three-dimensional chaotic system. *Nonlinear Dyn.* **67**, 335343 (2012).
- [22] Saif F.: Dynamical localization and signatures of phase space. *Phys. Lett. A* **274**, 98-103 (2000). Saif F., Riedel K., Schleich W.P. and Mirbach B., *Dynamical Localization and Decoherence*. Published in: *Lecture Notes in Physics, Decoherence: Theoretical, Experimental, and Conceptual Problems*, Eds.: Ph. Blanchard, D. Giulini E. Joos C. Kiefer and I.-O. Stamatescu, 179-189 (Springer, Heidelberg, 2000).
- [23] S. Fishman, Grepel, D. R., Prange, R. E., *Phys. Rev.*

- Lett. **49**, 509 (1982).
- [24] R. Blümel et al. Phys. Rev. A **44**, 4521 (1991).
- [25] F. L. Moore *et al.*, Phys. Rev. Lett. **73**, 2974 (1994).
- [26] P. J. Bardroff et al., Phys. Rev. Lett. **74**, 3959 (1995).
- [27] Saif F., Bialynicki-Birula I., Fortunato M., and Schleich W.P.. Fermi Accelerator in Atom Optics. Phys. Rev. A **58**, 4779-4782 (1998).
- [28] A. Schelle, Dominique Delande, and Andreas Buchleitner Phys. Rev. Lett. **102**, 183001 (2009).
- [29] P. Meystre, Ann. Phys.(Berlin) **525**, 215 (2013).
- [30] R. Blumel *et al.*, Nature (London) **334**, 309 (1988); M. Moore, R. Blumel, Phys. Rev. A **48**, 3082 (1993).
- [31] J. Esteve *et al.*, Nature (London) **455**, 1216 (2008); F. Brennecke, *et al.*, *ibid*, **450**, 268 (2007).
- [32] F. Brennecke, S. Ritter, T. Donner, T. Esslinger, Science **322**, 235 (2008).
- [33] C. K. Law, Phys. Rev. A **51**, 2537 (1995).
- [34] C. W. Gardiner, *Quantum Noise* (Berlin, Springer, 1991).
- [35] M. Paternostro, S. Gigan, M. S. Kim, F. Blaser, H. R. Böhm, and M. Aspelmeyer, New Journal of Physics **8**, 107 (2006).
- [36] V. Giovannetti, D. Vitali, Phys. Rev. A **63**, 023812 (2001).
- [37] T. J. Kippenberg and K. J. Vahala, Optics Express , 17172 (2007).
- [38] T. Carmon, H. Rokhsari, L. Yang, T. J. Kippenberg, and K. J. Vahala, Phys. Rev. Lett. **94**, 223902 (2005).
- [39] T. Carmon, M. C. Cross, and K. J. Vahala, Phys. Rev. Lett. **98**, 167203 (2007).
- [40] A. Ottl, S. Ritter, M. Kohl, and T. Esslinger Rev. Sci. Instrum. **77**, 063118 (2006).
- [41] F. Brennecke1, T. Donner, S. Ritter, T. Bourdel, M. Kohl, T. Esslinger, Nature (London) **450**, 268 (2007)
- [42] M. El Ghafar et al., Phys. Rev. Lett. **78**, 4181 (1997).